Nanotechnology Perceptions
ISSN 1660-6795
www.nano-ntp.com

Investigation of Mn and Fe/Co-Doped ZnO Nanocrystalline: Examining Synthesis, Structure, and Ferromagnetism at Room Temperature

Sanjay Kumar[1], Virendra Kumar[2], Manoj Kumar Bansal[3], Piyush Dua[4]

[1]GL Bajaj Institute of Technology &Management, Greater Noida, India
[2]Ajay Kumar Garg Engineering college, Ghaziabad, India
[3]Bharat Institute of Technology, Meerut, India
[4]Department of Applied Sciences, DBS Global University, Dehradun, Uttarakhand, India

In this article, we report Pristine ZnO (zinc Oxide) and synthesis of its doped variants with Mn and Fe i.e. (Zn)0.985(Mn).015O (manganese doped zinc Oxide) and (Zn)0.985(Fe).015O (iron doped zinc Oxide) by solid-state reaction method. The structural, morphological, optical, and magnetic properties of the prepared samples were investigated. The crystalline, hexagonal wurtzite phase of pure ZnO (Zinc Oxide) and its doped compositions were discovered by XRD (Xray diffractometer). SEM images reveal that pure ZnO (Zinc Oxide) doped with Mn and Fe were in the nanoscale range having a size of 20-100nm.Findings of Raman spectra for Mn doped variant indicates that the mode at 496 cm-1 is attributed to a local Mn-related vibrational mode. The mode at 695cm-1 ought to be a ZnO intrinsic mode and attributed to the E1 longitudinal optical spectrum. UV study of the samples confirms that the energy band gap (Eg) decreases from 2.92 eV to 2.72eV for Mn-doped and up to 3.37eV for Fe-doped compositions. This decrease may be attributed to the domination of dopant ions in the composition. The M-H curves for the samples (Zn)0.985(Mn).015O and (Zn)0.985(Fe).015O depicts the induction of Superparamagnetic in these compositions. An examination of magnetic properties showed a shift from the diamagnetic nature of pure ZnO to room-temperature ferromagnetic behavior in doped samples. The current research successfully achieved room-temperature ferromagnetism in Mn and Fe/Co doped ZnO nanoparticles, presenting a promising option for real-world applications in the future.

Keywords: X-ray diffraction, ZnO nanoparticles, Dielectric properties, Magnetic properties, Optical properties.

1. Introduction

ZnO is a well - known wide band gap semiconducting (3.37 eV) material having wurtzite

structure with lattice parameter a = b = 0.325 nm and c = 0.5206 nm (1). ZnO is tetrahedral synchronized and assembled through the c-axis. (2-3). Based on the size-dependent, electronic and optical properties, pristine Zinc oxide and its various doped compositions with transition metals have been widely studied in the last one and half decade. The research interest in ZnO was also triggered due to its applications in optoelectronics because of its direct wide band gap (3.3ev) at room temperature. Though ZnO was discovered few decades ago and recently many research groups have worked on ZnO to enhance its various properties (6-9). Apart from this ZnO is also an appropriate material for Sensors, optoelectronics, and Energy storage devices (4-5). Moreover, ZnO is also a propitious candidate for spintronics (28) and Super paramagnetism (31-32).Due to high potential in Industrial and technological sector multidisciplinary research has been carried out to target various aspects of pure and doped ZnO. The various research groups have confirmed by their studies that ZnO doped with transition metals i.e. Mn and Fe has a substantial impact on its various properties [38]. It is also reported that n-type ZnO shows a adequately long (Room Temperature) spin-coherence time and it is also possible to dope ZnO either as a p or n-type semiconductor having low resistivity. ZnO has been provided as a pragmatic course of action for bipolar spintronics materials. As far as ingenious magnetic ground state of the ZnO is concerned, It has been shown that how the doping of Mn at desired site of triangular network can affect its magnetic properties (33)

Taking into consideration the above cited research work was appropriate for us to reinvestigate the effect of transition metals (Mn, Fe) on magnetic behavior of ZnO. Apart from this we also investigated this doping effect on various optical properties of ZnO, which are not studied much in earlier reporting's. Moreover, this present research of ours which represents effect of doping of transition metals on ZnO would be useful for the futuristic optoelectronic devices.

2. Experimental Details

(Zn)0.985(Mn).015O (abbreviated as ZMnO) Manganese doped zinc oxide and (Zn)0.985(Fe).015O (abbreviated as ZFeO) Iron doped zinc oxide were synthesized by mixing Mn and Fe in appropriate ratio in pristine ZnO by using solid state reaction route. We used high purity oxides of above mentioned materials which were mixed with isopropanol. The constituent materials were blazed at 7000C for 11 hours after mixing. Phase identification and structural analysis was carried out by x-ray diffractometer (Smart lab SE Rigaku) having CuKα radiations of wavelength λ = 1.54056 A0 with the scan rate 0.2/min for 2θ range from 20 to 80 degree. The microstructures of the specimen were investigated with the help of Scanning Electron Microscope (FE-SEM Nova Nano SEM 450).For elemental analysis EDAX (Quantex EDX Bruker) was used. For magnetic measurements vibrating sample magnetometer (VSM Lakeshore 7304) was used. The ferroelectric loop tracer (Marine India) was used to study ferroelectric behaviour of prepared samples.

3. Results and discussions

3.1 XRD Analysis

Phase identification and the structural analysis was carried out for pristine, manganese

doped(Zn)0.985(Mn).015O (abbreviated as ZMnO) and iron doped manganese doped zinc oxide (Zn)0.985(Fe).015O (abbreviated as ZFeO) with the help of x-ray diffractometer (XRD) with 2θ range from 20 to 80 which is shown in Fig.1. There is no impression of any impurity peaks in recorded XRD pattern, which is also established by the JCPDS card No.250330.The bulk density of pure and doped ceramic samples was calculated with the help of micromeritics instrument (provided by Mettlier toledo India). The estimate of bulk density for pristine ZnO is 3.52×103 Kg/m3 and for Mn and Fe doped variants of ZnO are 3.56×103Kg/m3 and 3.58×103 Kg/m^3 respectively. These analysis of bulk density indicate that after adding Mn and Fe content the absorbency of prepared samples decreases as shown in table no.1.The lattice parameters were calculated by the following equations.

$$a = \frac{\lambda}{\sqrt{3}\ \sin\theta}\sqrt{h^2 + hk + k^2} \quad (1)$$

$$\text{and} \quad c = \frac{\lambda}{2\ \sin\theta}\ell \quad (2)$$

Where λ is the wavelength,θ is the angle of diffraction, and (h,k,l) are miller indices. The volume of the unit cell was calculated by the mathematical relation

$$V = \frac{\sqrt{3}}{2}a^2c = 0.866a^2c \quad (3)$$

Where V is the volume of lattice, a and c are the lattice constants.

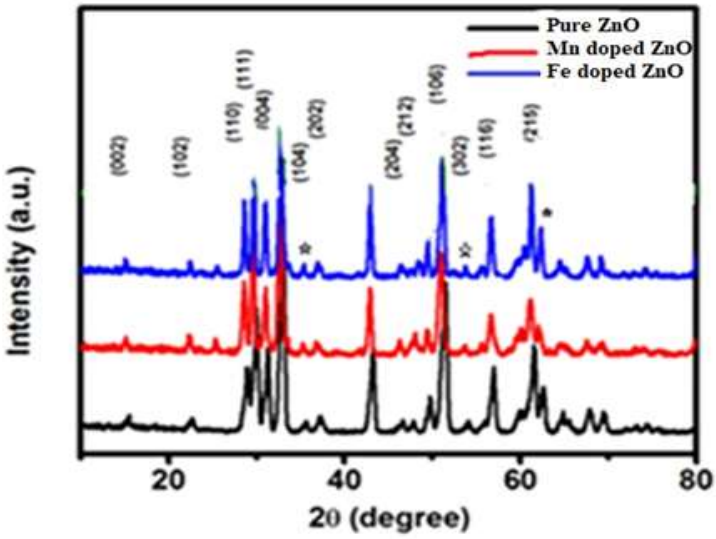

Figure.1 X-ray diffraction pattern for pristine, manganese doped $(Zn)_{0.985}(Mn)_{.015}O$ and iron doped $(Zn)_{0.985}(Fe)_{.015}O$

Table -1 indicates the lattice parameters as well as cell volume (V) obtained from XRD patterns. The lattice parameters calculated are a=b= 3.2488A0, c = 5.2056 A0 for pure ZnO and 3.2468A0, 5.2106A0, for Mn, 3.2473A0, 5.2067A0 for Fe doped samples, respectively. The obtained cell volume is a 47.55 A0, for pristine ZnO, 47.54A0 and 47.52A0 for Mn and Fe doped samples respectively.

Table 1: XRD Peak positions, crystallite size and cell volume for pristine, manganese doped $(Zn)_{0.985}(Mn)_{.015}O$ and iron doped $(Zn)_{0.985}(Fe)_{.015}O$.

Values of x	Peak position ($2\Theta^0$)	Average Crystallite size(nm)	Cell Parameters	Lattice Parameters			Cell volume
				a = b	c	c/a	V(Å^3)
ZnO	36.32	51.39	2.4713	3.2488 A^0	5.2056 A^0	1.605	47.55
$(Zn)_{0.985}(Mn)_{.015}O$	36.27	52.32	2.4742	3.2468 A^0	5.2106 A^0	1.601	47.54
$(Zn)_{0.985}(Fe)_{.015}O$	36.27	51.37	2.4744	3.2473 A^0	5.2067 A^0	1.602	47.52

3.2. SEM and EDX analysis

Scanning Electron Micrographs (SEM) ahead with Elemental X-ray diffraction analysis (EDAX) spectra for (Zn)0.985(Mn).015O (abbreviated ZMnO) and (Zn)0.985(Fe).015O (abbreviated as ZFeO) are depicted in Fig. 2. The average grain sizes of the samples are calculated with the help of line intercept method which comes out to be between 20-25µ. EDAX spectra of ZnO doped with Mn and Fe is shown in Fig. 2(a-c) along with SEM micrographs. (EDAX) spectra of pristine and its Mn and Fe doped ZnO variants show the occupancy of oxygen, Zink and Manganese in the sample and the corresponding intensities of O, Zn and Mn are in agreement with their varying weight percentage in the composition. The reciprocal ferocity peaks of pristine ZnO and its doped variants are also clearly distinguished.

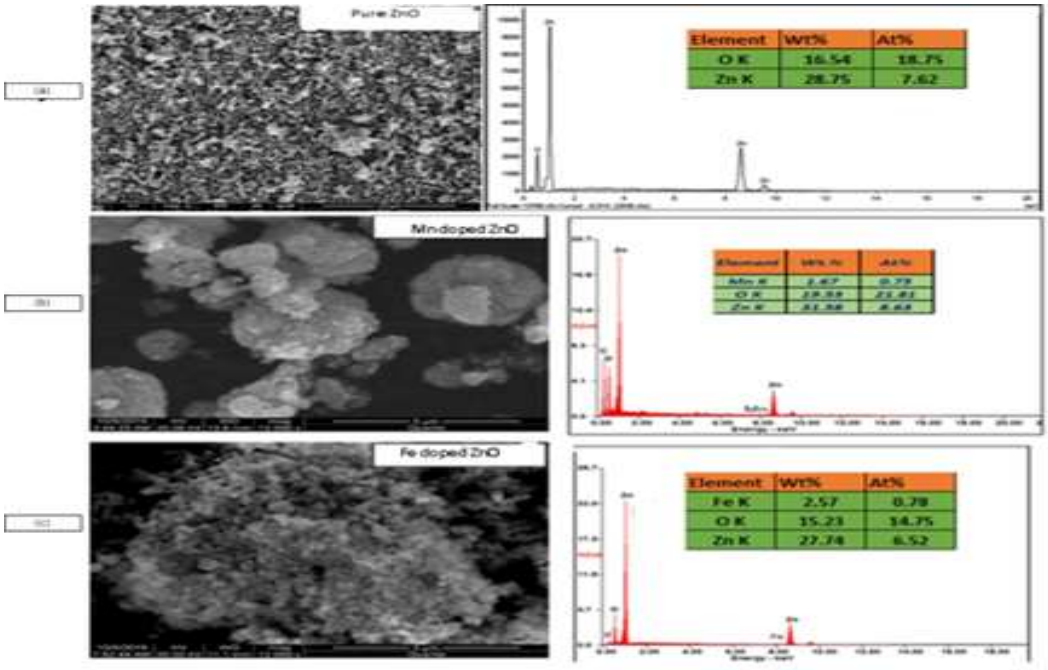

Figure.2 SEM micrograph and the corresponding EDS spectrum for pristine, manganese doped $(Zn)_{0.985}(Mn)_{.015}O$ and iron doped $(Zn)_{0.985}(Fe)_{.015}O$

3.3 Raman analysis

The Raman Spectra of (Zn)0.985(Mn).015O (abbreviated as ZMnO)and(Zn)0.985(Fe).015O (abbreviated as ZFeO) along with pristine ZnO is shown in Fig.3.Obtained spectra reveal five

peaks at 132,307,367,496 and 628 cm-1. It is clear from the Fig3,that even if most of the Raman peaks of Mn and Fe doped be consistent with those of pure ZnO. The band is composed of peaks 132 and 307 cm-1extricated by Lorentz fitting. The key attributes is that the intensity of the 307 cm-1 mode decreases delinquently to the potential variations of the composite chaos.

Raman Spectra for) pristine, manganese doped (Zn)0.985(Mn).015O (abbreviated as ZMnO) and iron doped (Zn)0.985(Fe).015O (abbreviated as ZFeO).

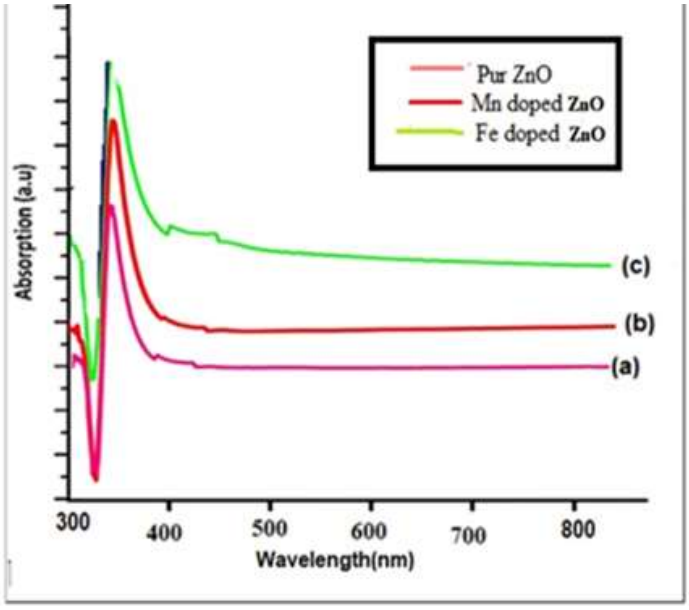

Figure.3 Raman Spectra for) pristine, manganese doped $(Zn)_{0.985}(Mn)_{.015}O$ and iron doped $(Zn)_{0.985}(Fe)_{.015}O$

3.4. UV-visible analysis

Optical absorption of (Zn)0.985(Mn).015O (abbreviated as ZMnO) and (Zn)0.985(Fe).015O (abbreviated as ZFeO) along with pristine ZnO as a function of wavelength are shown in Fig. 4. It is measured by using the UV-Visible optical spectroscopy in the range in between (300-800nm). It is confirmed from that the assimilation peak increases after Mn and Fe doping in pure ZnO. The increment in absorbance may be due to abundant feature like, particle size, oxygen deficiency and imperfection in gain structure. The vigorous absorbance is achieved for the wavelength below 380 nm, while a very stubby absorbance is observed in the visible region. It is clear from graph that band structure and change in absorption peaks take place due to various dopants. The transpose of the engrossment boundary constituted the exchange in the particle energy gap. It should be understood that the depletion in energy gap, is related to enhance effectiveness of the application of materials in optoelectronics appliances.

The direct band gaps for pristine and Mn, Fe doped ZnO were calculated by the Tauc's plot relation as given below [37].

$$(\alpha h\upsilon) = c\,(h\upsilon - Eg) \qquad \text{-------} \qquad (4)$$

Where αthe absorption coefficient constant, h plank is's constant, υ is the frequency of photons and Eg is the energy band gap.

Figure .4 UV-Vis Spectra for pristine, manganese doped $(Zn)_{0.985}(Mn)_{.015}O$ and iron doped $(Zn)_{0.985}(Fe)_{.015}O$

The band gap of pristine ZnO and its doped variants are 2.92eV, 2.73eV and 2.72eV respectively are shown in Fig.5. The energy band gap for pristine ZnO decreases after doping with Mn and Fe. This may be due to the imperfections (cation or anion vacancies) which are created after the doping. Mithal et al. and Mazhdi et al.[35]

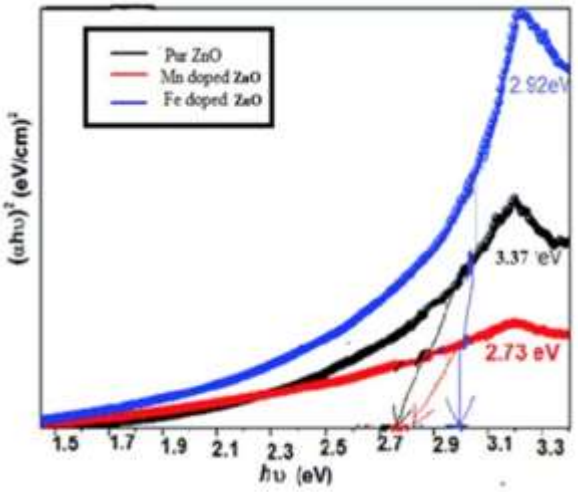

Figure.5 The Energy band gaps for pristine, manganese doped $(Zn)_{0.985}(Mn)_{.015}O$ and iron doped $(Zn)_{0.985}(Fe)_{.015}O$

3.5. P-E Loops analysis

Ferroelectric loops are depicted in Fig.6 having (Zn)0.985(Mn).015O (abbreviated as ZMnO) and (Zn)0.985(Fe).015O (abbreviated as ZFeO) at room temperatures. A constant field is applied before measurement of samples. Loops of Mn and Fe doped ZnO compositions reposition themselves towards negative field axis. This elongated behavior can be corresponding to the passive layer emergence at the ferroelectric /substructure electrode coherence. As far as the coercive electric field and remnant polarization is concerned for Pristine ZnO its value lies (2Pr ~.526μc/cm2) and (2Ec ~6.22Kv/cm). After doping, the value of coercive electric field and remnant polarization decreases for Mn and Fe doped samples i.e. (2Pr ~ 0.181μc/cm2), (2Ec ~3.12Kv/cm) and (2Pr ~ 0.171μc/cm2), (2Ec ~ 2.13Kv/cm) respectively.

Figure.6 Room temperature ferroelectric loops for pristine, manganese doped $(Zn)_{0.985}(Mn)_{.015}O$ and iron doped $(Zn)_{0.985}(Fe)_{.015}O$

Table2: Different experimentally observed parameters for pristine, manganese doped $(Zn)_{0.985}(Mn)_{.015}O$ and iron doped $(Zn)0.985(Fe)_{.015}O$

Values of x	Bulk density(Kg/m^3)	M_s(Saturation magnetization)	P_f(Remnant polarization) $\mu c/cm^2$	E_C(Coercive field) kV/cm
ZnO	3.52×10^3	0.024	0.526	6.22
$(Zn)_{0.985}(Mn)_{.015}O$	3.56×10^3	0.073	0.181	3.12
$(Zn)_{0.985}(Fe)_{.015}O$	3.58×10^3	0.083	0.171	2.13

3.6. M-H Curve analysis

This advancement in ferroelectric behavior can be corresponding to magnetic endowment as compared to electric polarization. Electric polarization would be jumped from one group of state to the other. After doping, ferroelectric behavior may be improved as compared to room temperature paramagnetic nature is concerned. After doping, the diamagnetic ZnO exhibit paramagnetic behavior after doping with Mn and superparamagnetic nature after doping with Fe.

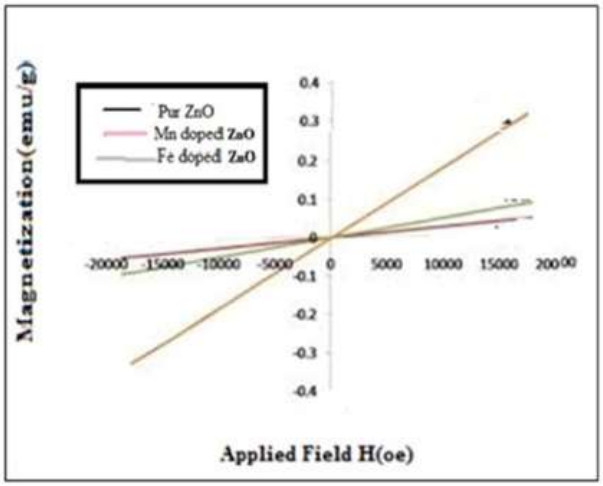

Figure.7 M-H Curve for pristine, manganese doped $(Zn)_{0.985}(Mn)_{.015}O$ and iron doped $(Zn)_{0.985}(Fe)_{.015}O$

4. Conclusions

(Zn)0.985(Mn).015O (abbreviated as ZMnO) and (Zn)0.985(Fe).015O (abbreviated as ZFeO) were amalgamate by solid state reaction method. The XRD patterns disclose the wurtzite structure for all the nano-samples and no degradation phase was distinguished. The maximum translucent size obtained from XRD was less than 100nm. The average grains size obtained from SEM measurement for prepared samples is in between 20-25μm. We have also determined that the optical and magnetic properties of ZnO are greatly improved using the optimal delighted of ZnO doped with Mn and Fe. The energy bands of Mn and Fe are 2.73 eV and 2.92, respectively. The M-H curve revealed the absence of ferromagnetic behavior. In the present work, Structural, Morphological, Magnetic and Optical Properties of Mn and Fe doped

ZnO Nanoparticles are improved by the solid state reaction method. This study is valuable for producing transition metal-doped ZnO nanoparticles that exhibit enhanced optical and magnetic properties, making them suitable for various spintronics applications.

Funding Details

This work was supported by Ajay Kumar Garg Engineering college, Ghaziabad,India

Disclosure Statement

This is to acknowledge any financial interest or benefit that has arisen from the direct applications of your research.

References

1. Yu, H.; Chen, Y.; Wei, W.; Ji, X.; Chen, L. A Functional Organic Zinc-Chelate Formation with Nanoscaled Granular Structure Enabling Long-Term and Dendrite-Free Zn Anodes.
2. (1) Pan, P.; Chen, X.; Xing, H.; Deng, Y.; Chen, J.; Alharthi, F. A.; Alghamdi, A. A.; Su, J. (2021),A fast on-demand preparation of injectable selfhealing nanocomposite hydrogels for efficient osteoinduction. Chin. Chem. Lett. 32, 2159−2163.
3. Tomboc, G. M.; Zhang, X.; Choi, S.; Kim, D.; Lee, L. Y. S.; Lee, K. (2022) Stabilization, Characterization, and Electrochemical Applications of High-Entropy Oxides: Critical Assessment of Crystal Phase−Properties Relationship. Adv. Funct. Mater., 32, No. 2270242.
4. Darvishi, E.; Kahrizi, D.; Arkan, E. (2019) Comparison of different properties of zinc oxide nanoparticles synthesized by the green (using Juglans regia L. leaf extract) and chemical methods. J. Mol. Liq., 286, No. 110831.
5. Kanwal, S.; Khan, M. T.; Mehboob, N.; Amami, M.; Zaman, A. (2022)Room-temperature ferromagnetism in Cu/Co Co-doped ZnO nanoparticles prepared by the co-precipitation method: for spintronics applications. ACS Omega, 7, 32184−32193.
6. Shirsath, S. E.; Wang, D.; Jadhav, S. S.; Mane, M. L.; Li, S. (2018) Ferrites obtained by sol-gel method. Handb. Sol-Gel Sci. Technol., 695−735.
7. Zaman, A.; Uddin, S.; Mehboob, N.; Ali, A. (2020) ,Structural investigation and improvement of microwave dielectric properties in Ca (HfxTi1-x) O3 ceramics. Phys. Scr. 96, No. 025701.
8. Husain, S.; Alkhtaby, L. A.; Giorgetti, E.; Zoppi, A.; Miranda, (2014) M. M. Effect of Mn doping on structural and optical properties of sol gel derived ZnO nanoparticles. J. Lumin., 145, 132−137.
9. Guo, Y.; Cao, X.; Lan, X.; Zhao, C.; Xue, X.; Song, Y. (2008) Solutionbased doping of manganese into colloidal ZnO nanorods. J. Phys. Chem. C, 112, 8832−8838
10. C.F. Klingshirn, B.K. Meyer, A. Waag, A. Hoffmann, J. Geurts, et .al (2010). Zinc Oxide: From Fundamental Properties towards Novel Applications. Springer Series in Materials Science, Springer, Berlin.
11. C. W. Bunn, Proc. Phys. (1935) Soc. London et .al: 7-835
12. H. Braekken and CJore, Det Norske (1935)Videnskabers Skrifter the Norwegian Science Scripts NR8, in Norwegian et .al:1-4.
13. R. B. Heller, J. McGannon, and A. H. Weber et .al (2004) .J. Appl. Phys:1-21
14. T. B. Rhymer and G. D. Archard et .al (1952). Research London .
15. A. Cimino, M. Marezio, and A. Santoro, Natures. et .al (1957): 1-12
16. T. J. Gray, et .al J. (1954) .Am. Ceram. Soc:2-5
17. G. P. Mohatny and L. V. Azaroff, et .al (1961) . J. Chem. Phys:1268
18. A. A. Khan, Acta Crystallography. Sect. A: et .al (1968) Cryst.Phys. Diffr. Theor.
19. Gen.Crystallography: 24-40

20. R. R. Reeber, et .al., (1970). J. Appl. Phys) :41
21. D. C. Reynolds and T. C. Collins, et .al (1969) . Phys. Rev:185
22. D. G. Thomas, et .al (1960). J. Phys. Chem. Solids, :15
23. Y. S. Park, C. W. Litton, T. C. Collins, and D. C. Reynolds, et .al (1965). Phys. Rev:143
24. R. J. Collins and D. A. Klein man, et .al (1959). J. Phys. Chem. Solids:11
25. R. L. Weiher, et .al (1966). Phys. Rev:152
26. W. S. Bear, et .al (1967) Phys. Rev:154
27. E. Mollwo, Z. Angew. et .al (1954). Phys: 6
28. W. L. Bond, et .al (1965) J. Appl. Phys:36
29. W. Y. Liang and A. D.Yoffe, et .al (1968) . Phys. Rev. Lett:20,
30. A. R. Hutson, et .al (1961). J. Appl. Phys:32
31. J. L. Freeouf, Phys. et .al (1973). Rev. B: 7
32. O. F. Schirmer and D. Zwingel, et .al (1970). Solid State Common:8
33. J. J. Hopfield and D. G. Thomas, et .al (1965). Phys. Rev. Lett.:22
34. R. E. Stephens and I. H. Malitson, et .al (1952) . J. Res. Natl. Bur. Stand:49
35. Y. S. Park and J. R. Schneider, et .al (1968) . J. Appl. Phys:39
36. G. Heiland, E. Mollwo, and F. Stöckmann, et .al (1959). Solid State Phys:191
37. D. C. Look, D. C. Reynolds, J. W. Hemski, R. L. Jones, and J. R. Sizelove, et .al (1999). Appl. Phys. Lett:811
38. A. Y. Polyakov et al. et .al (2003).J. Appl. Phys.:94
39. S. O. Kucheyev, J. S. Williams, C. Jagadish, J. Zou, C. Evans, A. J. Nelson, and A. V. Hamza, et .al (2003) .Phys. Rev. B:67
40. T. Dietl, H. Ohno, F. Matsukura, J. Cibert, and D. Ferrand, et .al (2000). Science :1019
41. S. J. Pearton et al., et .al (2004). J. Phys.: Condens. Matter:16,
42. S. J. Pearton, W. H. Heo, M. Ivill, D. P. Norton, and T. Steiner, Semicond. Sci. Technol. et .al (2004):19
43. C.-T. Lee, et .al (2010) . Fabrication Methods, and Luminescent Properties of ZnO Materials for Light Emitting Diodes, Materials:3
44. [34] D. Mithal and T. Kundu, et .al (2017). Effect of Gd3+ doping on structural and optical properties of ZnO nanocrystals, Solid State Sci:68
45. [35] M. Mazhdi and M. Tafreshi, The effects of gadolinium doping on the structural, morphological,optical, and photoluminescence properties of zinc oxide nanoparticles prepared by co-precipitation method, et .al (2018) Appl. Phys. A: Mater. Sci. Process:124
46. B. D. Cullity, Introduction to Magnetic materials. et .al (1972). Addision-Wesley. London:388
47. Tauc J in S Nudelman and S Mitra (eds) et .al (1966) .Optical properties and electronic structure of Amorphous semiconductors (Boston: Springer US)
48. Han, C.; Duan, L.; Zhao, X.; Hu, Z.; Niu, Y.; Geng, W. et .al (2019).Effect of Fe doping on structural and optical properties of ZnO films and nanorods. J. Alloy. Compd: 854–863.